MULTI-PARAMETER NLFM PULSE COMPRESSION WAVEFORM DESIGN TO ADDRESS LOW TIME-BANDWIDTH PRODUCT CONSTRAINTS

Alexander C van Zyl[1], Erich A Wiehahn[2], Jacques E Cillers[3], Thomas R Niesler[4]

[1]Stellenbosch University, Stellenbosch, South Africa
[2]Stellenbosch University, Stellenbosch, South Africa
[3]CSIR, Pretoria, South Africa
[4]Stellenbosch University, Stellenbosch, South Africa

Keywords: PULSE COMPRESSION, NON-LINEAR FM (NLFM), PEAK SIDELOBE (PSL), BÉZIER, LOGIT

Abstract

Radar literature contains numerous publications on Non-Linear Frequency Modulated (NLFM) waveforms where the majority of the modulation functions are either implemented assuming the radar can afford to have a large Time-Bandwidth Product (TBP) or make use of mathematical operations that are difficult to parameterise. This allows them to perform well at a high TBP, but poorly at a low TBP where commercial off the shelf (COTS), short-range and low power Software-Defined Radio (SDR) based radars operate. These radars have limited bandwidth due to the low sampling rates and the problem becomes worse when transmitting at short distances in scenarios where pulsed operation is required. This paper compares some waveforms and develops a multi-parameter, optimisable NLFM waveform based on Bézier curves. It is shown that the Bézier and logit based waveforms outperform the waveforms used for comparison.

1 Introduction

The chosen Pulse Compression (PC) waveform in a radar has a substantial effect on the target detection performance. This is due to the variation in the response of the PC stage in the signal processing pipeline. The resultant Main Lobe Width (MLW) affects the range resolution and the Peak Side-Lobe (PSL) level affects the detection of low Radar Cross-Section (RCS) targets in the presence of high RCS targets. Both of these variables can be adjusted by modification of the transmitted waveform and/or modification of the receive PC filter. Many of these techniques result in a mismatch between the transmit and receive waveform which, in turn, causes a SNR loss relative to the theoretical maximum SNR gain which can be achieved for a given TBP.

Numerous waveforms have been developed [1]-[3] the majority of which revolve around certain assumptions and mathematical operators. It is therefore difficult to add parameters to the process due to the mathematical nature of these designs. In addition to this, if the radar breaks the assumptions made in the design process it is not going to perform as expected. One of these assumptions is that the radar operates in the high TPB regime, which is the case in most high performance, long-range, radars. However, in a COTS, short-range, SDR based radar the TBP is highly constrained. It is therefore necessary to develop a waveform that is not based on the abovementioned assumption made regarding the TBP.

2 Reference Waveforms

In order to measure the waveform's performance, some are chosen for comparison. Linear Frequency Modulation (LFM) is used as a baseline since it is the most basic form of modulation. The LFM waveform has the drawback that its sidelobe performance is poor, with the first sidelobe being 13 dB below the peak. A NLFM waveform presented by Leśnik [1] is used as the comparison to a mathematically developed NLFM waveform that performs well at a high TBP. Logit and sinh are used for their simplicity and ability to be parameterised using a single control parameter.

2.1 Linear Frequency Modulation

The LFM waveform is given by

$$f(n) = \exp(j2\pi f_w n), \tag{1}$$

$$f_w = \frac{f_{BW}}{N-1} n - \frac{f_{BW}}{2}, \tag{2}$$

where N is the number of samples and f_{BW} is the bandwidth of the signal.

2.2 Leśnik NLFM

Leśnik [1] proposes a NLFM waveform that is calculated using the Zak transform. The signal is given by

$$s(t) = A\text{rect}\left(\frac{t - \frac{t_i}{2}}{t_i}\right)\exp(j2\pi\theta(t)), \tag{3}$$

$$\theta(t) = \frac{t_i\sqrt{\Delta^2+4}}{2\Delta} - \left(\frac{{t_i}^2(\Delta^2+4)}{4\Delta^2} - \left(t - \frac{t_i}{2}\right)^2\right)^{\frac{1}{2}}, \tag{4}$$

where Δ is the total instantaneous frequency change and t_i is the total transmission time.

2.3 Logit

The logit is the inverse of the popular sigmoid function. It is presented in this paper in a normalised and centred form where it can be easily manipulated using one parameter. It is given by

$$f(x) = -m\ln((c_1x + c_2)^{-1} - 1), \quad x \in [-1, 1], \tag{5}$$

$$c_2 = \frac{1}{1 + e^{-\frac{0}{m}}} = 0.5, \tag{6}$$

$$c_1 = \frac{1}{1 + e^{-\frac{1}{m}}} - c_2, \tag{7}$$

$$m = e^{1-p}, \tag{8}$$

where p is the tuning parameter. A higher value of p corresponds to a higher non-linearity. It is scaled with Eq. 8 so that the linearity can scale linearly and a value of 0 corresponds to LFM.

2.4 Hyperbolic Sin

The hyperbolic sin (sinh) is also presented in a parametric form similar to the logit. It is given by

$$f(x) = m\sinh(cx), \quad x \in [-1, 1], \tag{9}$$

$$c = \sinh^{-1}\left(\frac{1}{m}\right), \tag{10}$$

$$m = e^{1-p}, \tag{11}$$

where p is the tuning parameter similar to the logit function.

2.5 Comparison

Fig. 1 compares the pulse compression of the different waveforms mentioned above. This figure presents some problems encountered when designing pulse compression waveforms. The Leśnik waveform does not perform as expected due to the difference in TBP compared to the paper where it is presented. Although both the sinh and logit waveforms are optimised for a low PSL, it is clear that their MLW are drastically different and this effect will be investigated further in the paper. In addition to this, these waveforms are very limited in their shapes and a more flexible waveform design methodology is required to yield better results.

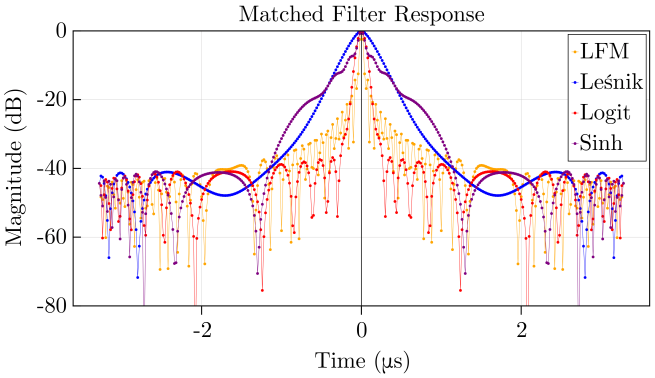

Fig. 1: A comparisson of the waveforms' pulse compression. Both the logit and sinh is optimised for a low PSL at a TBP of 66 (bandwidth = 20Mhz, transmission time = 3.33 μs and f_s = 50 MHz). The logit function parameter is 2.282 and the sinh parameter is 4.798.

3 Bézier Curves

Bézier curves [4] are presented as the solution to the multi-parameter problem. It is a technique that is regularly used in computer graphics environments to define a curve using a series of vertices and has previously been applied to radar waveform design in [5] & [6]. The number of vertices can be changed, allowing for the development of a waveform design technique that allows a varying amount of parameters. The baseline is a Bézier with three vertices, at (-1,-1), (0,0) and (1,1), giving a normalised LFM waveform. Conjugate vertices can now be added to increase the complexity and non-linearity of the modulation.

The explicit form of the Bézier curve is given by

$$B(t) = \sum_{i=0}^{n}\binom{n}{i}(1-t)^{n-i}t^iP_i, \tag{12}$$

where P_i is the vertex describing the Bézier curve and n is the order of the curve, which is one less than the number of vertices. For the initial investigation a 4^{th} order Bézier curve is used, allowing one to plot the parameter space in 3 dimensions since the x and y coordinates of only one vertex are varied. This vertex is reflected from the positive frequency quadrant to the negative frequency quadrant to enforce symmetry in the time-frequency curve.

The first step is to calculate the PSL level of the waveform as the Bézier vertex is varied. A surface plot of these results can be seen in Fig. 2. It is highly non-linear due to the side lobes merging with the main lobe as the vertex varies, causing the algorithm to ignore the merged side lobe since it has effectively become the main lobe. The side-lobe adjacent to the merged one is now regarded as the new PSL, hence the sudden

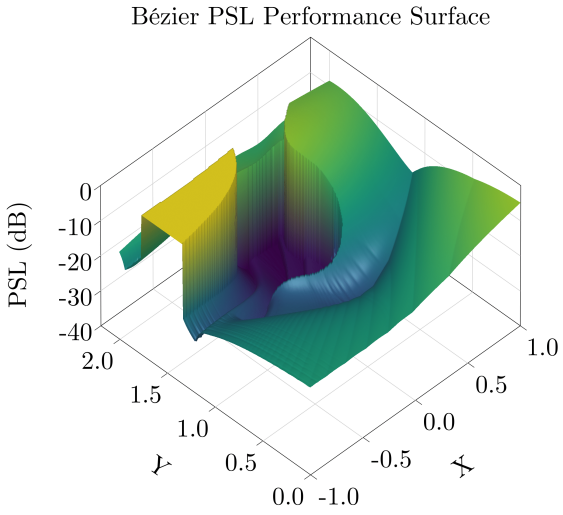

Fig. 2: The PSL of a 4^{th} order Bézier waveform with varying positions. The waveform has the same specifications as those in Fig. 1.

discontinuity. It is therefore also necessary to include the zero-to-zero (0-0) MLW to have enough information to optimise the waveform.

The 0-0 MLW plot can be seen in Fig. 3 and is also highly non-linear for the same reasons mentioned for the PSL plot. To gain a better understanding of the effect of the Bézier vertex on the MLW and PSL both plots are overlayed in a contour plot in Fig. 4.

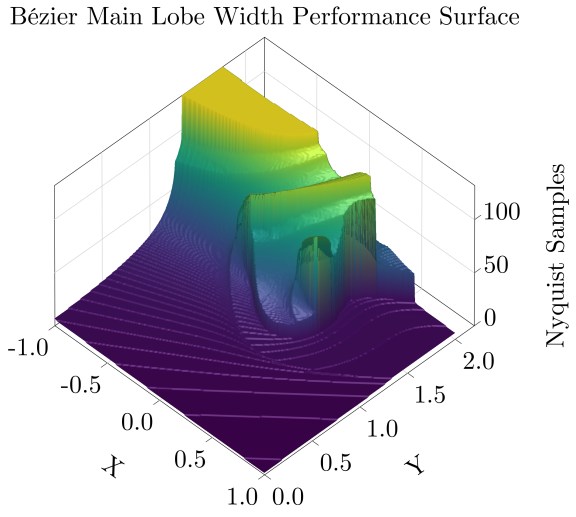

Fig. 3: The main lobe width of a 4^{th} order Bézier waveform with varying positions. The waveform has the same specifications as those in Fig. 1.

From Fig. 4 there is an area where the PSL drops drastically, but to reach that area the MLW has to be increased. Upon further investigation of the 4^{th} order Bézier curve, it is clear that it is not capable of generating high-performance waveforms. The parameter space, as seen in Fig. 5, shows it is not able to surpass the logit waveform. It is therefore necessary to investigate the performance of higher-order Bézier curves. This requires optimisation since the parameter space scales exponentially.

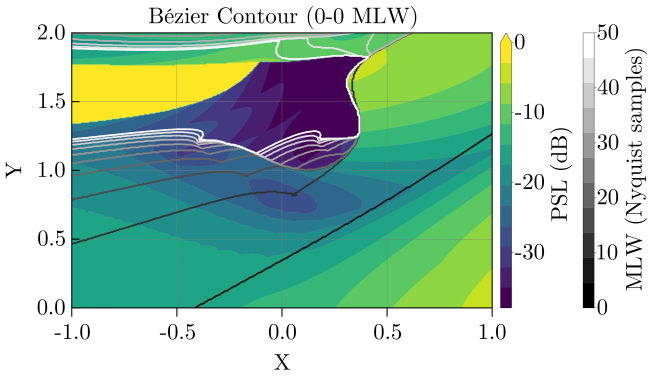

Fig. 4: The PSL (Fig. 2) and MLW (Fig. 3) plots overlayed as contour plots.

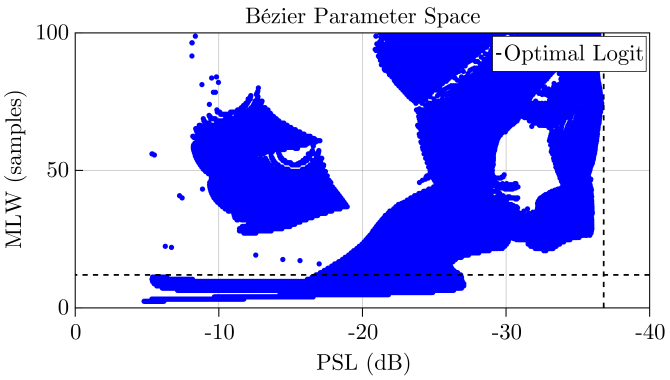

Fig. 5: The parameter space (x and y coordinates are varied) for a 4^{th} order Bézier curve. The logit (optimised for PSL) is shown for reference.

4 Optimisation

Coordinates for the vertices of the Bézier curve resulting in the minimisation of MLW and PSL must be determined to find an optimal waveform. This multi-objective optimisation problem has conflicting objectives; coordinates for vertices resulting in favourable values for the PSL often correspond to unfavourable values for the MLW (see Fig. 2 - 5). The fitness function given by Eq. 13 is used to combine the two objectives such that compatibility with single-objective optimisation methods is obtained.

$$\text{Fitness} = \alpha\text{PSL} + \frac{\beta}{\text{MLW}}, \quad \alpha \in (-\infty, 0), \tag{13}$$

The fitness function is non-convex, non-smooth and potentially high-dimensional. Furthermore, derivatives with respect

to the coordinates of Bézier curves are not available. Gradient-based optimisation methods, *i.e.* stochastic gradient descent, are therefore not appropriate. Derivative-free optimisation methods that broadly emulate gradient descent such as the Nelder-Mead method [7] are prone to get stuck in local minima and are thus not recommended for non-convex functions [8]. Brute force techniques become increasingly unfeasible for higher-order Bézier curves due to a combinatorial explosion of problem complexity.

Taking the aforementioned characteristics into consideration, particle swarm optimisation (PSO) [9] was chosen to maximise the fitness function. Each particle in the swarm is incentivised to explore the search space by means of an attraction factor towards the best position visited by itself while concurrently being drawn to better regions via an attraction factor towards the best global position visited by any particle in the swarm. Particles can often navigate non-convex fitness functions without getting stuck on local maxima by retaining momentum during position updates. PSO is implemented in Julia [10] using Optim.jl [11] within an optimisation framework provided by Hyperopt.jl [12].

The optimiser was run at the same specifications as the waveforms in Fig. 1 and the results are presented in Fig. 7 and Tab. 1. The 4^{th} order waveform performs poorly, but there is a large increase in performance when going to the 6^{th} order waveform. Increasing the order further has little to no effect on the performance of the waveform at this TBP.

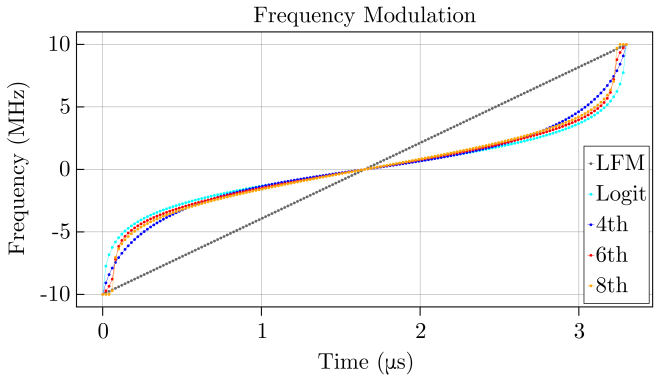

Fig. 6: The optimal frequency modulation for different orders of Bézier curves. The waveforms have the same specifications as those in Fig. 1.

5 Conclusion

The aim of this paper was to develop a NLFM waveform design methodology in the low TBP regime that is parameterised and can be optimised. Optimised Bézier curves were implemented as the solution and their MLW and PSL performance was investigated. From Tab. 1 it is clear that the Bézier outperforms the other waveforms used as reference. Further investigations can be done into optimising higher-order Bézier curves and comparing the results to more NLFM waveforms. Interestingly, the NLFM waveform based on the logit function exhibited

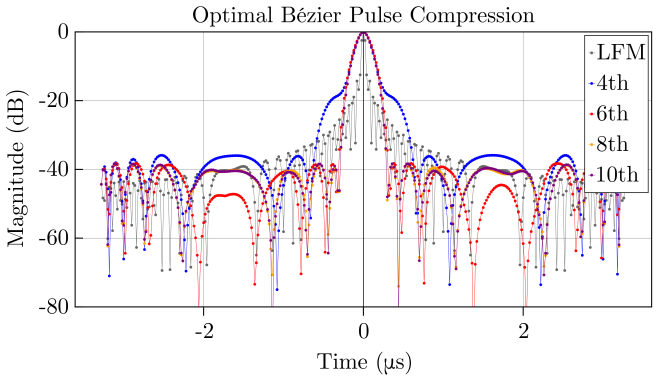

Fig. 7: Pulse compression output for the waveforms in Fig. 6.

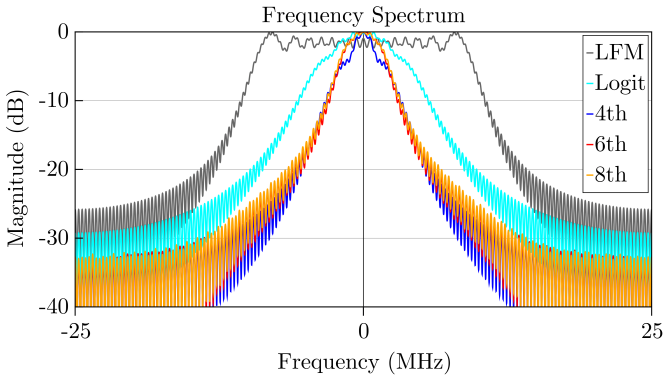

Fig. 8: The frequency spectrums for the waveforms in Fig 6.

Table 1
Performance metrics for various waveforms. All waveforms have a bandwidth of 20 MHz and transmission time of 3.33 μs. MLW is given when sampled at the Nyquist frequency.

Waveform	**PSL [dB]**	**MLW [samples]**
LFM	-14.29	2.4
Logit	-36.84	12
Sinh	-40.9	52
Leśnik	-41.1	68
Bézier (4^{th})	-35.89	26.4
Bézier (4^{th})	-27.45	6.4
Bézier (6^{th})	-38.26	12.8
Bézier (6^{th})	-37.85	12.0
Bézier (6^{th})	-36.81	9.6
Bézier (8^{th})	-38.47	12.0
Bézier (8^{th})	-38.10	11.2
Bézier (10^{th})	-38.31	12.0
Bézier (10^{th})	-38.16	11.2

MLW and PSL performance on par with the best Bézier based waveform.

6 Future Work

This paper reports on an active area of research and further results will be added to this paper as the research progresses.

Some areas of investigation will include extending the performance metrics to include the -3 dB MLW as well as integral metrics on the sidelobe region. The current analysis will be extended to include a spread of TBP values. Due to the fact that the spectra of the NLFM waveforms is narrow compared to that of the LFM waveform a utilised bandwidth measure, such as occupied bandwidth will also be added to the set of metrics used by the optimisation process.

7 Acknowledgements

Thank you to my family and friends for your continuing love and support.

8 References

[1] Leśnik, C.: 'Nonlinear Frequency Modulated Signal Design', Acta Physica Polonica A, September 2009, Vol. 116, pp. 351-.

[2] De Witte, E. and Griffiths, H.D.: 'Improved waveforms for satellite-borne precipitation radar', International Waveform Diversity & Design Conference, 2006, pp. 1-7.

[3] Doerry, A.: 'Generating precision nonlinear FM chirp waveforms', 2007.

[4] Mortenson, M.E.: 'Mathematics for Computer Graphics Applications', Industrial Press Inc, 1999, pp. 264.

[5] Kurdzo, J., Cheong, B.L., Palmer, R. and Zhang, G.: 'Optimized NLFM Pulse Compression Waveforms for High-Sensitivity Radar Observations', International Radar Conference, 2014.

[6] Kurdzo, J., Cho, J., Cheong, B.L. and Palmer, R.: 'A Neural Network Approach for Waveform Generation and Selection with Multi-Mission Radar', April 2019.

[7] Nelder, J.A. and Mead, R.: 'A Simplex Method for Function Minimization', The Computer Journal, 1965, Vol. 7, Issue 4, pp. 308–313.

[8] Sparks, E.R., Talwalkar, A., Haas, D., Franklin, M.J, Jordan, M.I. and Kraska, T.: 'Automating model search for large scale machine learning', Proceedings of the Sixth ACM Symposium on Cloud Computing, 2015, pp. 368-380.

[9] Kennedy, J. and Eberhart, R.: 'Particle swarm optimization.', Proceedings of ICNN'95-international conference on neural networks, 1995, Vol. 4, pp. 1942-1948.

[10] Bezanson, J., Edelman, A., Karpinski, S. and Shah, V. B.: 'Julia: A fresh approach to numerical computing', 2017, SIAM Review, 59(1), pp. 65–98.

[11] Mogensen, P.K. and Riseth, A.N.: 'Optim: A mathematical optimization package for Julia', Journal of Open Source Software, 2018, Vol. 3, No. 24, pp. 615.

[12] Bagge Carlson, F.: 'Hyperopt.jl: Hyperparameter optimization in Julia', 2018, GitHub, https://lup.lub.lu.se/search/publication/6ec19989-9b30-448c-be5e-bae4c4257c7b.